

# **Influence of Physical and Chemical Environments on the Decay Rates of $^7\text{Be}$ and $^{40}\text{K}$**

E. B. Norman, G. A. Rech, E. Browne, R.-M. Larimer, M. R. Dragowsky,

Y. D. Chan, M.C. P. Isaac, R. J. McDonald, and A. R. Smith

Nuclear Science Division, Lawrence Berkeley National Laboratory  
Berkeley, CA 94720 U.S.A.

## **Abstract**

We measured the electron-capture decay rate of  $^7\text{Be}$  implanted into hosts of graphite, boron nitride, tantalum, and gold. We have found that this decay rate varies by as much as 0.38% from one host to another. We also measured the electron-capture decay rate of  $^{40}\text{K}$  in four different chemical compounds and as both a solid and dissolved in solution. To within our measurement precision of  $\pm 1\%$ , we have found no influence of the environment on the  $^{40}\text{K}$  decay rate. The implications of these results for the solar neutrino problem and for potassium/argon dating are discussed.

PACS Numbers: 23.40.-s, 27.20.+n, 27.40.+z

Keywords: Be-7, K-40, electron-capture decay, gamma-ray spectroscopy

Corresponding author: Eric B. Norman

MS 50-208, Lawrence Berkeley National Laboratory, Berkeley, CA 94720, U.S.A.

E-mail: [EBNORMAN@LBL.GOV](mailto:EBNORMAN@LBL.GOV) Phone: 510-486-7846; FAX: 510-486-6738

## Introduction

Electron-capture decay rates depend sensitively on the density of atomic electrons within the nucleus. Thus, environmental factors such as pressure, chemical form, magnetic fields, etc. that can alter electron densities, may affect electron-capture decay rates. Over a period of many years, numerous experiments have been conducted to search for such effects in a variety of radionuclides, but almost all of the observed effects have been very small,  $\leq 0.1\%$  [1,2]. Recently, however, there have been several reports of surprisingly large variations (up to 1%) in the decay rate of  $^7\text{Be}$  as a function of the host material into which it was implanted [3,4] and as a function of pressure [5].

$^7\text{Be}$  is a good candidate in which to look for such variations because of its simple electronic structure:  $1s^2 2s^2$ , and the fact that approximately 10% of all electron-captures take place from the L shell [6]. Furthermore, the decay rate of  $^7\text{Be}$  is important for estimating the flux of neutrinos emitted by the Sun [7,8,9].  $^{40}\text{K}$  is another radionuclide for which environmental effects could be important. The electron-capture decay of  $^{40}\text{K}$  to the 1461-keV level in  $^{40}\text{Ar}$  is a first-forbidden-unique transition with a  $Q_{\text{EC}}$  of only 44 keV [6]. This decay mode is the basis for the potassium/argon dating technique. Apparent inconsistencies between ages deduced from  $^{40}\text{K}/^{40}\text{Ar}$  and U/Pb ratios for samples found at the Oklo natural reactor site [10] could be due to environmental effects on the electron-capture decay rate of  $^{40}\text{K}$  [11]. Because of their relevance in a number of important areas of science, we decided to carefully measure the decay rates of  $^7\text{Be}$  and  $^{40}\text{K}$  under several different conditions to look for variations in these quantities. We produced  $^7\text{Be}$ , implanted it into four different host materials, and then measured its decay rate. In a previous experiment, Norman *et al.* [12] searched for deviations

from the exponential decay law by comparing the decay rate of freshly-prepared  $^{40}\text{K}$  to that of  $4.5 \times 10^9$ -year old material. Within their experimental uncertainties, no such deviations were observed. In the present work, we measured the electron-capture decay rate of  $^{40}\text{K}$  in different chemical and physical forms.

## **$^7\text{Be}$ Experiments**

All of the  $^7\text{Be}$  samples were produced by irradiating targets with ion beams from Lawrence Berkeley National Laboratory's 88-Inch Cyclotron. For the samples in graphite and boron nitride, we produced and stopped the  $^7\text{Be}$  recoils in the target. The  $^7\text{Be}$  in graphite sample was made by bombarding a thick graphite target with 40-MeV  $^3\text{He}$  ions. The  $^7\text{Be}$  source in boron nitride was produced by bombarding a solid BN target with a beam of 10-MeV protons. For the  $^7\text{Be}$  sources in tantalum and gold, we used a different approach. A 60-pnA beam of 45-MeV  $^7\text{Li}$  ions irradiated a stack of three 0.076-mm thick Kapton ( $\text{C}_{22}\text{H}_{10}\text{O}_5\text{N}_2$ ) foils. The  $^7\text{Be}$  recoils produced by the  $^1\text{H}(^7\text{Li}, ^7\text{Be})\text{n}$  reaction escaped from the Kapton and were stopped in either a 0.025-mm thick Ta foil or a 0.018-mm thick Au foil located immediately behind the production target. The initial activities of the  $^7\text{Be}$  sources ranged from 0.8  $\mu\text{Ci}$  (for the boron nitride sample) to 5.7  $\mu\text{Ci}$  (for the graphite sample).

Following these irradiations, each  $^7\text{Be}$  source was packaged together with a 1- $\mu\text{Ci}$   $^{133}\text{Ba}$  reference source and rigidly mounted onto an individual polyethylene holder for subsequent counting. In order to reduce systematic errors from variations in source position, system dead time, or detector/electronics performance, we measured the decay rate of  $^7\text{Be}$  relative to that of  $^{133}\text{Ba}$ . A 110-cm<sup>3</sup> high-purity coaxial germanium detector surrounded by a graded shield of Al-

Cu-Cd-Pb was used to accumulate gamma-ray data in one-day intervals over 6-months. For counting, each  $^7\text{Be}/^{133}\text{Ba}$  sample was positioned 5.7-cm away from the endcap of the detector. Each  $^7\text{Be}/^{133}\text{Ba}$  sample was counted for a period of at least ten days and then the sample was changed.  $\gamma$ -ray spectra were accumulated using an ORTEC ACE PC-based data acquisition system. Precise time calibrations of the beginning of the counting were obtained by synchronizing the internal clock of the PC with standard time obtained from Pacific Bell Telephone Co. A typical one-day spectrum obtained from the gold sample is shown in Figure 1.

We extracted from each one-day bin the net peak area of the 478-keV  $^7\text{Be}$  gamma ray,  $N_\gamma(478)$ , and that of the 356-keV  $^{133}\text{Ba}$  gamma ray,  $N_\gamma(356)$ . This was done by integrating a suitably wide window centered on the full-energy peak and then subtracting from this result the average of two equally wide background windows chosen symmetrically above and below the peak. The statistical uncertainty in the net peak area was determined by combining in quadrature the uncertainty in the gross peak area and that of the average background area. The ratio,  $R = N_\gamma(478)/N_\gamma(356)$ , versus time was then fit to a single exponential decay function using a least-squares fitting procedure. The fractional statistical uncertainties in  $R$  were found to range from 0.07% to 0.50% per point, with most of them being on the order of 0.15% or less. The decay constant determined from each fit was then corrected for the decay of the  $^{133}\text{Ba}$  ( $t_{1/2} = 10.54$  years [6]) to obtain the half-life of  $^7\text{Be}$  in each of the host materials that we studied. The results of these fits and their residuals are shown in Figure 2.  $^7\text{Be}$  half-life values and their corresponding reduced chi-square results obtained for each host are summarized in Table 1.

Our measurements have shown that the half-life of  $^7\text{Be}$  does appear to depend on the host material in which it is located. The shortest half-life that we have found is for the graphite host and the longest is for the gold host. In order to demonstrate that there is a statistically

significant difference in the result we found for the gold sample, we performed the following test. We computed the un-weighted average of the half-lives obtained from the boron nitride, graphite, and tantalum hosts, 53.159 days, and then fitted the gold data with the half-life fixed at this value. The resulting  $\chi^2_v$  was found to be 1.33 as compared to 1.04 found when the half-life was allowed to vary freely to obtain the best possible fit. For the 48 data points we obtained from the gold sample this difference in  $\chi^2$  represents a  $3.7\sigma$  effect, and is strong evidence for a variation in the half-life of  $^7\text{Be}$  in gold as compared to that in the other host materials.

The decay constant of  $^7\text{Be}$  in gold,  $\lambda(\text{Au})$ , compared to that in graphite,  $\lambda(\text{C})$ , shows a difference of

$$[\lambda(\text{Au}) - \lambda(\text{C})] / \lambda(\text{C}) = (-0.38 \pm 0.09)\% \quad (1).$$

A similar comparison for tantalum gives

$$[\lambda(\text{Ta}) - \lambda(\text{C})] / \lambda(\text{C}) = (-0.17 \pm 0.11)\% \quad (2).$$

The qualitative trend of our results is the same as that obtained by Ray *et al.* [4] and opposite to that observed by Souza *et al.* [3]. Quantitatively, however, our result for the gold sample shows approximately half the effect seen by Ray *et al.* It might be thought that this difference could be explained by the choice of reference samples – graphite in our case and aluminum oxide for Ray *et al.* However, as can be seen in Table 1, two high-precision measurements of the half-life of  $^7\text{Be}$  in hosts of lithium fluoride [13] and aluminum [14] yielded values in very good agreement with each other and with those that we obtained from the graphite and boron nitride hosts. Thus, the quantitative discrepancy between our results and those of Ray *et al.* is most likely not due to the choice of reference samples, although its origin remains an open question. Our result for the tantalum sample shows that this decay rate may be slightly lower than that for graphite.

However, it clearly disagrees both in sign and magnitude with the approximately 1% higher

decay rate in tantalum observed by Souza *et al.* The origin of this discrepancy remains an open question.

### **<sup>40</sup>K Experiments**

In order to search for variations in the decay rate of <sup>40</sup>K with the chemical environment in which the <sup>40</sup>K is located, we purchased from Johnson Matthey Corp. the following four potassium compounds (all stated by the manufacturer to be “greater than 99.998% pure”): KCl, K<sub>2</sub>SO<sub>4</sub>, KNbO<sub>3</sub>, and KTaO<sub>3</sub>. The plan for this experiment was to measure the emission rate of the 1461-keV <sup>40</sup>K gamma-ray and then divide this quantity by the mass of <sup>40</sup>K contained in the sample to obtain its specific activity in each chemical compound. In order to reduce systematic errors associated with the counting of relatively large samples for long periods, we mixed a measured amount of each potassium compound with a known amount of 99.99% pure La<sub>2</sub>O<sub>3</sub>. By counting such a mixture of materials, we determined the emission rate of the 1461-keV  $\gamma$ -ray relative to that of the 1436-keV gamma-ray produced by the decay of the naturally-occurring long-lived radionuclide <sup>138</sup>La ( $t_{1/2} = 1.06 \times 10^{11}$  years [6]).

To prepare each sample for counting, we carefully weighed out approximately 25 grams of the potassium compound under study and approximately 150 grams of the La<sub>2</sub>O<sub>3</sub>. These materials were then thoroughly mixed in a plastic bottle. This mixture was then spooned into a pre-weighed plastic box and sealed for counting. Each sample was placed directly against the front face of an 80% relative efficiency low-background high-purity coaxial germanium detector that was surrounded by a copper and lead shield. The counting was performed in Lawrence Berkeley National Laboratory’s Low Background Facility. Each sample was counted for approximately 5 days in order to achieve 0.3% statistical uncertainty in the ratio of the 1461- to

the 1436-keV gamma-ray peak areas. Data were accumulated using an ORTEC ACE PC-based data acquisition system. The relevant portion of the gamma ray spectrum observed from the  $\text{KTaO}_3 + \text{La}_2\text{O}_3$  mixture is shown in Figure 3.

The results of these measurements are summarized in Table 2. For each potassium compound, the ratio of the 1461- to the 1436-keV gamma ray emission rates,  $R_\gamma(1461)/R_\gamma(1436)$ , both estimated from the sample masses and measured directly in the gamma-ray counting are shown. All of the results have been normalized to those obtained from the  $\text{K}_2\text{SO}_4 + \text{La}_2\text{O}_3$  sample. The last column lists the ratios between these quantities determined from these two different techniques. If there were no variation in the specific activity of  $^{40}\text{K}$  with the chemical form of the sample, these numbers should all be 1.000. The observed departures from 1.000 seemed much too large to be attributed to effects of the chemical environment, and thus prompted us to further investigate the so-called “purity” of our potassium compounds.

We used the technique of neutron activation analysis (NAA) to determine the amount of potassium actually contained in each of our potassium compounds. The  $^{41}\text{K}(n,\gamma)$  reaction produces  $^{42}\text{K}$  which decays with a 12.4-hour half-life and emits a 1525-keV gamma ray. The  $^{139}\text{La}(n,\gamma)$  reaction produces  $^{140}\text{La}$ , which decays with a 40.3-hour half-life and emits a 1597-keV gamma ray. Thus, by neutron-irradiating a known mixture of the potassium compound under study and  $\text{La}_2\text{O}_3$  and then measuring the ratio of these two  $\gamma$ -ray peak areas, one can assay the relative potassium content of each compound.

We used a  $^{238}\text{Pu}/^9\text{Be}$  ( $\alpha,n$ ) source that emits approximately  $10^8$  neutrons/second to irradiate our samples. For each of our potassium compounds, 20-26 grams of the material under study and 1 gram of  $\text{La}_2\text{O}_3$  were carefully weighed and then mixed together. (Note that prior to weighing, each of these samples was baked at  $115^\circ\text{C}$  for 1.5 hours in order to drive off

any water that might have been contained in these materials.) Each such mixture was sealed in a plastic bag and then placed into a Lucite holder for irradiation. The neutron irradiations each lasted for approximately 18 hours, after which each sample was counted for 24 hours using the same germanium detector that was used in the direct gamma counting of the unirradiated materials. A portion of one of the gamma-ray spectra observed from the neutron-irradiated  $\text{KNbO}_3 + \text{La}_2\text{O}_3$  sample is shown in Figure 4.

The results of this NAA are summarized in Table 3. For each sample, the ratio of the numbers of  $^{41}\text{K}$  and  $^{139}\text{La}$  atoms,  $R^* = N(^{41}\text{K})/N(^{139}\text{La})$ , estimated from the measured sample masses and determined from the NAA, are shown. All of the results have been normalized to those obtained from the  $\text{K}_2\text{SO}_4 + \text{La}_2\text{O}_3$  sample. The last column lists the ratios of these quantities determined from the two different techniques. If all of these potassium compounds were actually “greater than 99.998% pure”, then the numbers in the last column would all be 1.000. The fact that they are not all 1.000 demonstrates that these potassium compounds are not as “pure” as claimed. Using the NAA results to determine the amount of potassium per unit mass in these compounds, one can divide the results of the direct  $\gamma$ -counting (shown in Table 2) by those shown in Table 3 to obtain the relative specific activity of  $^{40}\text{K}$  in these four different chemical forms. The results of this analysis are shown in Table 4.

We performed two additional experiments to search for the influence of the environment on the  $^{40}\text{K}$  decay rate. In the first experiment, we searched for a variation in the electron-capture decay rate of  $^{40}\text{K}$  in two different physical forms: solid and in solution. To do this test, we carefully weighed out and thoroughly mixed 50 grams each of dried  $\text{KCl}$  and  $\text{LaCl}_3$  powders. This mixture of solids was then  $\gamma$ -counted using an upward-looking coaxial germanium detector. The ratio of the areas of the 1461- ( $^{40}\text{K}$ ) and 1436-keV ( $^{138}\text{La}$ ) peaks was measured to be  $5.396 \pm$



0.030. This sample was then dissolved in approximately 500 ml of de-ionized water. The resulting solution was poured into a Marinelli beaker and then placed over the same germanium detector for counting the decays of the *same* atoms of  $^{40}\text{K}$  and  $^{138}\text{La}$ . The ratio of the  $^{40}\text{K}/^{138}\text{La}$  peak areas was found to be  $5.369 \pm 0.024$  from this liquid sample. The ratio of these quantities is then  $1.005 \pm 0.007$ .

The final experiment we did was to measure the rate of 1461-keV  $\gamma$ -ray emission from the *same*  $^{40}\text{K}$  atoms in two different chemical forms. To do this test, we carefully weighed out 113.3 grams of “high-purity”  $\text{K}_2\text{CO}_3$  and placed it into a plastic box. This sample was gamma counted with a coaxial germanium detector for one day. The observed counting rate of the 1461-keV  $^{40}\text{K}$   $\gamma$  ray was  $272.2 \pm 0.5$  counts/minute. This potassium carbonate was then dissolved in de-ionized water and converted into potassium chloride by slowly adding approximately 200 ml of concentrated HCl to the solution. The solution was boiled and then baked overnight to dryness. The resulting KCl powder was trituated using a mortar and pestle and then placed into a new plastic box. We weighed the KCl and found that we had recovered 99.0% of the potassium that was in the original  $\text{K}_2\text{CO}_3$ . The KCl was counted in the same geometry as was the  $\text{K}_2\text{CO}_3$ . The observed 1461-keV counting rate was  $270.2 \pm 0.5$  counts/minute. After correcting for the 1% difference in the amounts of potassium in these two samples, the ratio of the counting rate observed from the  $\text{K}_2\text{CO}_3$  to that from the KCl becomes  $0.997 \pm 0.003$ .

## Conclusions

Our measurements of the decay rate of  $^7\text{Be}$  implanted in several host materials show changes of up to 0.38%. Ray *et al.* [4] have suggested that this effect is due to variations in the

partial ionization of  $^7\text{Be}$  resulting from the different electron affinities of the hosts. Although we have also observed variations, they are approximately half as large as those predicted by the model of Ray et al. The implication for solar neutrinos is that estimates of the  $^8\text{B}$  neutrino flux based on the laboratory measurements of the half-life of  $^7\text{Be}$  [7,8,9] may be too high by as much as 1%. The size of this possible correction is considerably smaller than the current experimental uncertainty in the rate for the competing  $^7\text{Be}(p,\gamma)^8\text{B}$  reaction. Thus, at present, the observed variations in the  $^7\text{Be}$  decay rate do not warrant changing the predictions for the flux of  $^8\text{B}$  solar neutrinos.

From all of our experiments on  $^{40}\text{K}$ , we have found no evidence that its electron-capture decay rate is dependent on the chemical environment. Any possible deviation ( $\Delta\lambda/\lambda$ ) is  $\leq 1\%$ . Thus, the basis of the  $^{40}\text{K}/^{40}\text{Ar}$  dating technique remains secure. The apparent discrepancies in the K/Ar and U/Pb ages of samples from the Oklo reactor site must have some other origin. We have also learned that even very “pure” commercially produced chemicals are not always what they claim to be.

### **Acknowledgements**

We wish to thank Maurice Goldhaber [11] for bringing our attention to the question of whether the  $^{40}\text{K}$  decay rate might depend on the chemical environment. This work was supported by the U. S. Department of Energy under contract number DE-AC03-76SF00098.

## References

- [1] G. T. Emery, *Ann. Rev. Nucl. Sci.* **22** (1972) 165.
- [2] H. P. Hahn, H. J. Born, and J. I. Kim, *Radiochim. Acta.* **23** (1976) 23.
- [3] D. Souza et al., *Bull. Am Phys. Soc.* **42** (1997) 1679 and Univ. of Massachusetts-Lowell Rad. Lab. Prog. Rept. (DOE/ER/40246-12, Oct. 1997) p. 16.
- [4] A. Ray *et al.*, *Phys. Lett. B* **455** (1999) 69.
- [5] L.-G. Liu and C.-A. Huh, *Earth Planet. Sci. Lett.* **180** (2000) 163.
- [6] E. Browne and R. B. Firestone, *Table of Radioactive Isotopes* (Wiley, New York, 1986).
- [7] J. N. Bahcall, *Phys. Rev.* **128** (1962) 1297.
- [8] J. N. Bahcall, *Phys. Rev. D* **49** (1994) 3923.
- [9] J. N. Bahcall, *Astrophys. J.* **467** (1996) 475.
- [10] F. Gautier-Lafaye, P. Stille, R. Bros, and R. Taieb, in: *Proc. 2<sup>nd</sup> Oklo Working Group Meeting* (Brussels, April 1992) ed. H. von Maravic, Commission of European Communities. Report EUR-14877 (1993), p. 57.
- [11] M. Goldhaber, private communication.
- [12] E. B. Norman *et al.*, *Phys. Lett. B* **357** (1995) 521.
- [13] M. Jaeger, S. Wilmes, V. Kolle, G. Staudt, and P. Mohr, *Phys. Rev. C* **54** (1996) 423.
- [14] F. Lagoutine, J. Legrand, and C. Bac, *Int. Journ. Appl. Rad. and Isotop.* **26** (1975) 131.

## Figure Captions

1. A typical gamma-ray spectrum obtained in a one-day counting period from the gold sample. The 478-keV  $^7\text{Be}$  peak and the 356-keV  $^{133}\text{Ba}$  peak are labeled. The unlabelled peaks in the spectrum are either other lines from  $^{133}\text{Ba}$  or room background.
2. The ratio,  $R = N_\gamma(478)/N_\gamma(356)$ , and the residuals,  $(R_{\text{expt}} - R_{\text{fit}})$ , to the fits obtained from each  $^7\text{Be}$  sample. (a) boron nitride (b) graphite, (c) tantalum, (d) gold.
3. A portion of the gamma-ray spectrum observed from 5 days of counting the  $\text{KTaO}_3 + \text{La}_2\text{O}_3$  mixture. The  $^{40}\text{K}$  and  $^{138}\text{La}$  gamma rays are labeled. Unlabeled peaks are produced by a small impurity of  $^{227}\text{Ac}$  in the lanthanum oxide.
4. A portion of a gamma-ray spectrum observed following the neutron-irradiation of the  $\text{KNbO}_3 + \text{La}_2\text{O}_3$  sample. Gamma-ray peaks from  $^{40}\text{K}$ ,  $^{42}\text{K}$ , and  $^{140}\text{La}$  decays are labeled.

Table 1. Half-life of  $^7\text{Be}$  in various host materials as determined from least-squared fits to our measured gamma-ray spectra. For comparison,  $^7\text{Be}$  half-lives previously measured in two other hosts are also shown.

| Host                          | $t_{1/2}$ (days)   | $\chi^2_\nu$ |
|-------------------------------|--------------------|--------------|
| Graphite                      | $53.107 \pm 0.022$ | 1.25         |
| Boron Nitride                 | $53.174 \pm 0.037$ | 1.13         |
| Tantalum                      | $53.195 \pm 0.052$ | 1.11         |
| Gold                          | $53.311 \pm 0.042$ | 1.04         |
| <hr/>                         |                    |              |
| Lithium Fluoride <sup>a</sup> | $53.12 \pm 0.07$   |              |
| Aluminum <sup>b</sup>         | $53.17 \pm 0.02$   |              |
| <hr/>                         |                    |              |

<sup>a</sup> M. Jaeger *et al.* (Ref. 13)

<sup>b</sup> F. Lagoutine *et al.* (Ref. 14)

**Table 2. Comparison of  $^{40}\text{K}/^{138}\text{La}$   $\gamma$ -ray emission rates expected from measured sample masses versus those directly measured in  $\gamma$ -ray counting. All of the results have been normalized to those obtained from the  $\text{K}_2\text{SO}_4 + \text{La}_2\text{O}_3$  sample.**

| Sample  | $R = R_\gamma(1461)/R_\gamma(1435)$ |                       | $R(\text{Mass})/R(\gamma\text{-counting})$ |
|---|-------------------------------------|-----------------------|--|
|   | (Mass)                              | ( $\gamma$ -counting) |  |
| $\text{K}_2\text{SO}_4 + \text{La}_2\text{O}_3$ | 1.000                               | 1.000                 | 1.000                                      |
| $\text{KCl} + \text{La}_2\text{O}_3$            | 1.1655                              | $1.111 \pm 0.004$     | $0.953 \pm 0.004$                          |
| $\text{KNbO}_3 + \text{La}_2\text{O}_3$         | 0.4778                              | $0.3911 \pm 0.0011$   | $0.818 \pm 0.003$                          |
| $\text{KTaO}_3 + \text{La}_2\text{O}_3$         | 0.3163                              | $0.3108 \pm 0.0011$   | $0.983 \pm 0.004$                          |

**Table 3. Comparison of  $R^* = N(^{41}\text{K})/N(^{139}\text{La})$  expected from measured sample masses versus those determined by neutron activation analysis (NAA). All of the results have been normalized to those obtained from the  $\text{K}_2\text{SO}_4 + \text{La}_2\text{O}_3$  sample.**

| Sample  | $R^* = N(^{41}\text{K})/N(^{139}\text{La})$ |                   | $R^*(\text{mass})/R^*(\text{NAA})$ |
|---|---|-------------------|------------------------------------|
|   | (Mass)                                      | (NAA)             |                                    |
| $\text{K}_2\text{SO}_4 + \text{La}_2\text{O}_3$ | 1.000                                       | 1.000             | 1.000                              |
| $\text{KCl} + \text{La}_2\text{O}_3$            | 1.394                                       | $1.311 \pm 0.007$ | $0.941 \pm 0.005$                  |
| $\text{KNbO}_3 + \text{La}_2\text{O}_3$         | 0.7332                                      | $0.594 \pm 0.004$ | $0.810 \pm 0.005$                  |
| $\text{KTaO}_3 + \text{La}_2\text{O}_3$         | 0.3445                                      | $0.339 \pm 0.003$ | $0.984 \pm 0.009$                  |

**Table 4. Specific activity of  $^{40}\text{K}$  determined from direct  $\gamma$  counting,  $R$ , divided by the relative potassium content of the sample as determined by NAA,  $R^*$ . This quantity is proportional to the  $^{40}\text{K}$  electron capture decay constant. All of the results have been normalized to those obtained from the  $\text{K}_2\text{SO}_4$  sample.**

| <b>Sample</b>           | <b><math>R/R^* [\propto \lambda(^{40}\text{K})]</math></b> |
|-------------------------|--|
| $\text{K}_2\text{SO}_4$ | 1.000  |
| KCl                     | $1.013 \pm 0.007$  |
| $\text{KNbO}_3$         | $1.010 \pm 0.007$  |
| $\text{KTaO}_3$         | $0.999 \pm 0.010$  |



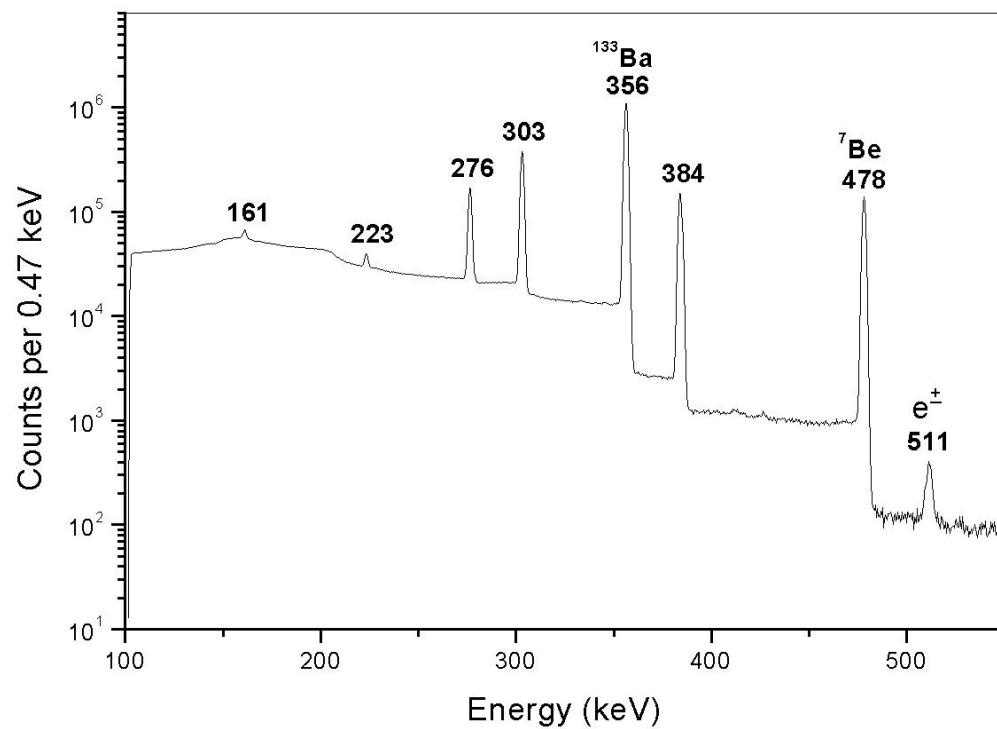


Figure 1

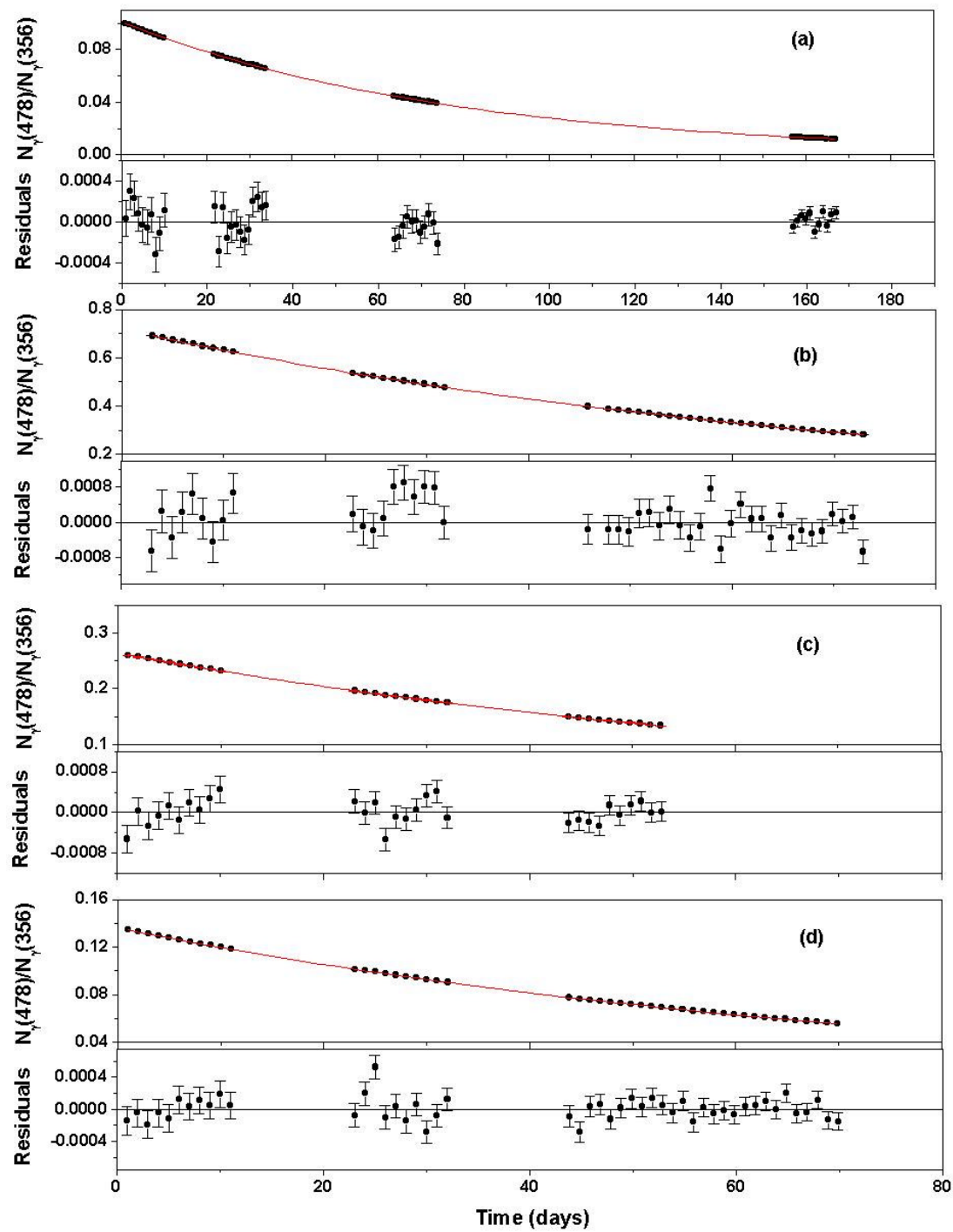


Figure 2

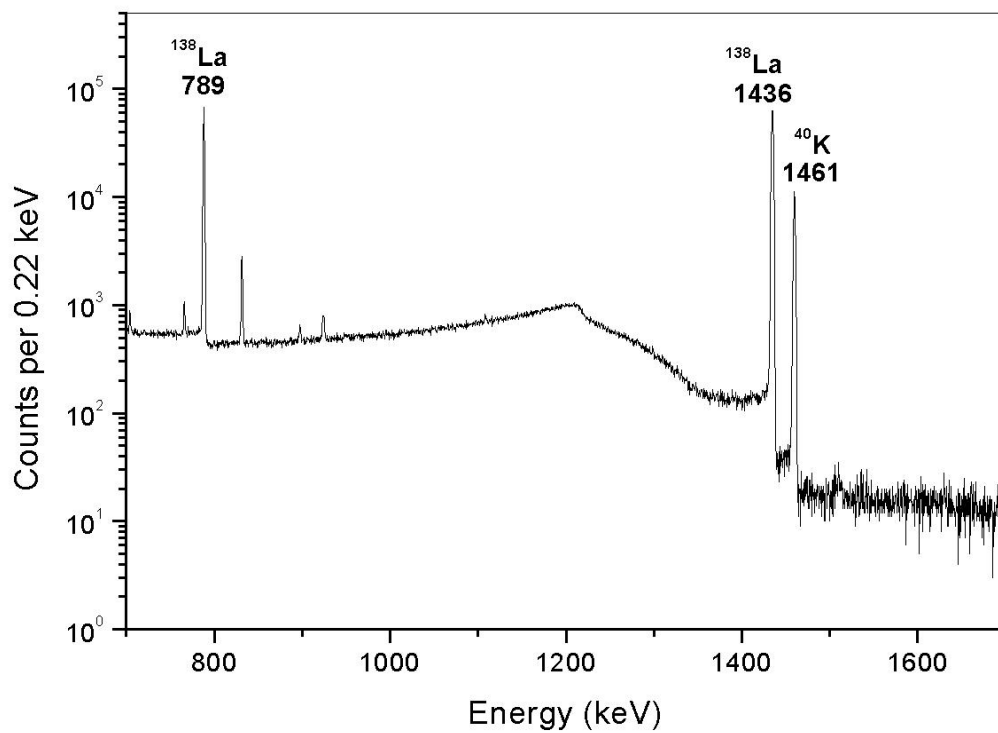


Figure 3

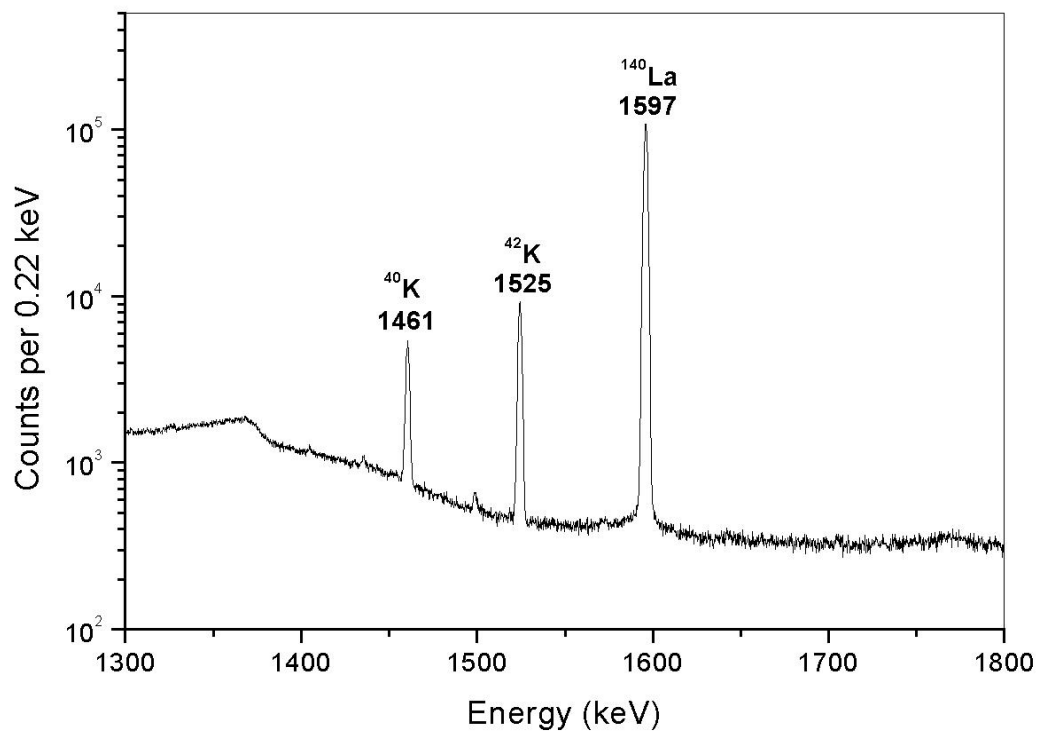


Figure 4